

12

Branchings in the s -channel and shadowing

We have a serious task ahead: to analyse and sum up the branchings, taking into account how they influence each other, and to learn how to write the amplitudes respecting unitarity.

12.1 Reggeon branchings from the s -channel point of view

12.1.1 The s -channel approach

In Lecture 2 we discussed how, given a particle spectrum, we can construct interaction amplitudes with the help of unitarity conditions and analyticity (dispersion relations). The dispersive method is well formulated and straightforward but not very convenient in practice. So instead of iterating the amplitudes through the non-linear unitarity relations we draw series of Feynman diagrams which satisfies (at least term by term) the unitarity condition.

Now we face an opposite situation for the first time. We discovered the branchings and found the specific unitarity conditions they satisfy. Can we construct an effective field theory that would generate the reggeon unitarity conditions?

There are two ways of attacking the problem.

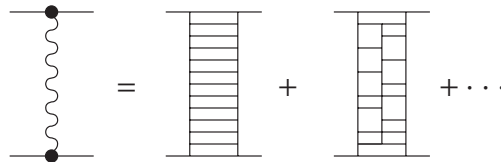
- (1) One can explicitly construct an effective reggeon QFT directly in the t -channel, identifying reggeons with particles of a non-relativistic (anti-hermitian) field theory in $2 + 1$ dimensions.
- (2) Alternatively, we can solve the problem of constructing the reggeon diagrams which solve the unitarity conditions, working directly in the s -channel.

The two routes yield the same results. We will follow the second one, for a number of reasons.

First of all, the *t*-channel reggeon unitarity conditions we studied in Lecture 11 were derived for positive *t*; in particular, the two-reggeon unitarity condition holds above $t = 16\mu^2$. The information so obtained has to be continued to the region $t < 0$ that really interests us. Moreover, the analysis of the discontinuity δf_j includes drawing complicated contours and is rather involved. In turns out that in the physical *s*-channel region, $t < 0$, everything looks much simpler, and the contours are trivial.

Secondly, if we work in the *s*-channel and exploit the *s*-channel unitarity, the problem of negative signature factors essentially disappears as well.

What did the Regge poles look like in the *s*-channel? We have seen that the simplest perturbative model for a pole was the *ladder*. From the point of view of the *t*-channel the ladder solves the two-particle unitarity condition. There are, of course, also corrections due to many-particle states in the *t*-channel.



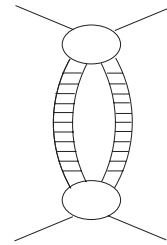
If we bear in mind the *exact* pole, rather than its naive perturbative image, it will contain everything.

Then, we considered a four-particle state and have accurately taken into account the interaction between particles (1) and (2), and (3) and (4), while neglecting cross-interactions between the pairs. This gave us a two-reggeon branch-cut singularity:

The equation (12.1) shows a diagrammatic relationship. On the left, a four-particle state is represented by two circles (vertices) connected by two wavy lines (reggeons). On the right, the same four-particle state is represented by two circles connected by a single wavy line. An arrow points from the left diagram to the right diagram, followed by an equals sign and the label (12.1).

The question is, what does this picture correspond to in the *s*-channel?

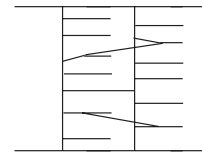
So, we have two ‘parallel ladders’. What we did here looks rather strange. Having suppressed cross-interactions in a four-particle state (which state in fact contributed to the *exact* pole) we obtained a *non-pole* singularity. To get it we had to pick some specific and, it seems, unimportant configurations when the usual strong interaction is not acting upon *all* the particles involved.



Recall that in perturbation theory the ladder diagram has emerged as the probability of a cascade production of many particles:

$$p_{01} \sim k_{01} \gg k_{02} \gg \dots \gg k_{0n} \sim m. \quad (12.2)$$

If I draw parallel cascades, momenta of particles from different chains will overlap, so that the two ‘combs’ may interact with each other, mixing everything in many ways. Squaring such an amplitude will produce a rather complicated picture.

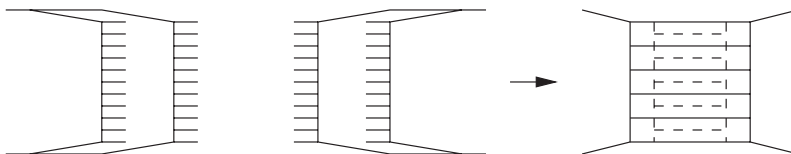


Certainly, by mixing up everything we would get a *large* contribution, even in perturbation theory. I hope, however, that this will be a contribution to the *pole*. Meanwhile, I want to find a particular piece, maybe not necessarily numerically large, but with *specific analyticity*.

Since in (12.2) particle momenta are gradually decreasing down the ladder, it is reasonable to expect that in our two-reggeon diagram (12.1) there are only particles with large momenta $k \sim p_1 \sim s/m$ in the upper block and small momenta $k \sim p_2 \sim m$ in the lower one (in the laboratory frame where the target particle p_2 is at rest).

12.1.2 Coexisting ladders – s -channel image of branching

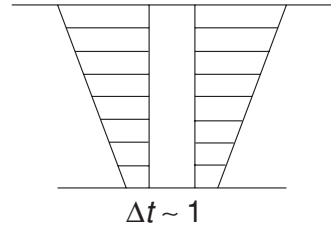
Once we decided to suppress the interaction between ‘combs’, I would draw the probability of such a process as follows:



In the s -channel we have *coexisting* ladders; from the t -channel point of view we have two separate (non-interacting) pairs of interacting

particles as shown in Fig. 12.1(a). The graph (a) has a particular *non-planar* topology. What about a simpler picture, also with two ladders, displayed in Fig. 12.1(b)? Will it also participate in the two-reggeon branching?

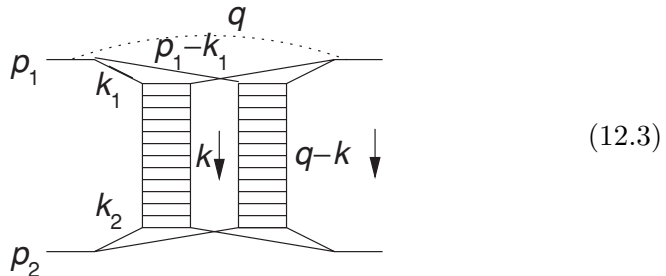
Let us ask ourselves, how does this process proceed in time? In the laboratory frame the slow target particle at the bottom of the graph gets the energy of the order of m so that the scattering process has to be over in a finite time $t = \mathcal{O}(m^{-1})$. But this implies that in a unit time the first fluctuation of the projectile has to collapse back, and the other one has to develop in order to assure the second interaction of the same fast particle with the target. Physically, it is impossible to arrange at such short notice. It is natural to expect therefore that the space-time configurations of the type of Fig. 12.1(b) will not contribute significantly in the high-energy limit. In what follows we will discuss in detail whether this is indeed the case.



We will devote the rest of this lecture to the investigation of the high-energy asymptotics of the diagram of Fig. 12.1(a), which we consider the main candidate for the *s*-channel image of the two-reggeon branching.

12.2 Calculation of the reggeon–reggeon branching

12.2.1 Kinematics and factorization



The diagram (12.3) contains three independent momentum integrations:

$$\begin{aligned}
 f_2 = & \frac{1}{2!} \int \frac{d^4k}{(2\pi)^{4i}} \int \frac{d^4k_1}{(2\pi)^{4i}} \int \frac{d^4k_2}{(2\pi)^{4i}} f_1(k_1, k_2, k) f_1(p_1 - k_1, p_2 - k_2, q - k) \\
 & \times \frac{1}{m^2 - k_1^2} \frac{1}{m^2 - (p_1 - k_1)^2} \frac{1}{m^2 - (k_1 - k)^2} \frac{1}{m^2 - (p_1 - k_1 - q + k)^2} \\
 & \times \left\{ \text{four lower-part propagators} \right\}.
 \end{aligned}
 \tag{12.4}$$

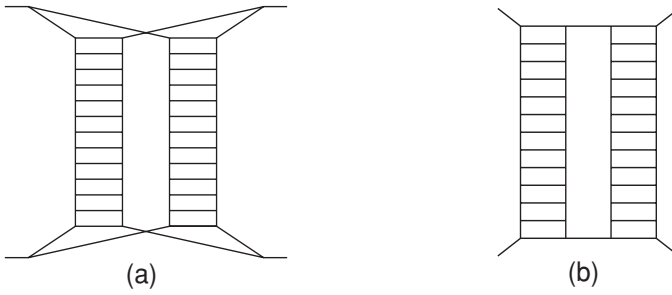


Fig. 12.1 Non-planar (a) and planar (b) two-ladder graphs.

We want to extract the contribution corresponding to the Regge poles in the ladder blocks f . The poles will appear, if the energy invariants of the ladders, $(k_1 + k_2)^2$ and $(p_1 - k_1 + p_2 - k_2)^2$, will tend to infinity in the $s \rightarrow \infty$ limit. In this asymptotics we hope to extract the contribution of the branching. We shall assume that the transverse momenta (and virtualities) of all participating particles stay finite,

$$\mathbf{k}_{i\perp}^2 \sim |k_i^2| = \mathcal{O}(m^2). \tag{12.5}$$

Introducing the usual Sudakov decomposition,

$$p_1^\mu = p_+^\mu + \gamma p_-^\mu, \quad p_2^\mu = \gamma p_+^\mu + p_-^\mu; \quad \gamma = \frac{m^2}{s},$$

we have

$$k_i^\mu = \alpha_i p_+^\mu + \beta_i p_-^\mu + k_{i\perp}^\mu; \quad (k_{i\perp}^\mu)^2 = -\mathbf{k}_{i\perp}^2.$$

Let us look at the propagators:

$$\begin{aligned} k_1^2 &= \alpha_1 \beta_1 s - \mathbf{k}_{1\perp}^2, \\ (p_1 - k_1)^2 &= (1 - \alpha_1)(\gamma - \beta_1)s - \mathbf{k}_{1\perp}^2. \end{aligned}$$

Applying the restriction (12.5) gives for the Sudakov components of k_1

$$|(p_1 - k_1)^2| \sim 2p_1 k_1 \sim \beta_1 s \sim m^2,$$

so that

$$\beta_1 = \mathcal{O}(m^2/s), \quad \alpha_1 = \mathcal{O}(1). \tag{12.6a}$$

This means that the offspring move almost parallel to the direction of the incident particle p_1 , sharing its large momentum in a finite proportion: $k_1 \simeq \alpha_1 p_1$, $(p_1 - k_1) \simeq (1 - \alpha_1)p_1$.

Considering analogously the bottom part of the graph,

$$\begin{aligned} k_2^2 &= \alpha_2 \beta_2 s - \mathbf{k}_{2\perp}^2 = \mathcal{O}(m^2), \\ (p_2 - k_2)^2 &= (\gamma - \alpha_2)(1 - \beta_2)s - \mathbf{k}_{2\perp}^2 = \mathcal{O}(m^2), \end{aligned}$$

we arrive at

$$\beta_2 = \mathcal{O}(1), \quad \alpha_2 = \mathcal{O}(m^2/s). \quad (12.6b)$$

Now we analyse the momentum transferred along the first ladder,

$$k^\mu = \alpha_k p_+^\mu + \beta_k p_-^\mu + k_\perp^\mu.$$

From the finiteness of the propagators exiting the ladder we get

$$\begin{aligned} (k_1 - k)^2 &\sim (\alpha_1 - \alpha_k)(\beta_1 - \beta_k)s = \mathcal{O}(m^2) \Rightarrow |\beta_k| \sim m^2/s, \\ (k_2 + k)^2 &\sim (\alpha_2 + \alpha_k)(\beta_2 + \beta_k)s = \mathcal{O}(m^2) \Rightarrow |\alpha_k| \sim m^2/s. \end{aligned} \quad (12.7)$$

This shows that the momentum transfer is practically *transversal* to the scattering plane:

$$k^2 = \alpha_k \beta_k s - \mathbf{k}_\perp^2 \simeq -\mathbf{k}_\perp^2, \quad (q - k)^2 \simeq -(\mathbf{q} - \mathbf{k})_\perp^2,$$

where we have used $|\alpha_q| \simeq |\beta_q| \simeq |q^2|/s = \mathcal{O}(m^2/s)$.

Since $|\alpha| \ll \alpha_1$, $|\beta| \ll \beta_2$, we can omit in all the propagators at the top part of the graph the α component of the momentum transfer and, correspondingly, β in the bottom. Then we observe that, thanks to the kinematical conditions (12.6), the integration variables have *factorized*:

$$\begin{aligned} \text{top propagators: } &\alpha_1, \beta_1, \beta_k; \\ \text{bottom propagators: } &\alpha_2, \beta_2, \alpha_k. \end{aligned} \quad (12.8)$$

12.2.2 High-energy behaviour

The ladder amplitude f depends on the invariant energy of the pair of particles that enter the ladder, on the momentum transfer and four virtual particle ‘masses’, e.g.

$$f_1 = f((k_1 + k_2)^2, k^2; k_1^2, (k_1 - k)^2, k_2^2, (k_2 - k)^2). \quad (12.9)$$

We observe that in our kinematics the invariant energies are of the order of the total energy indeed:

$$s_I \equiv (k_1 + k_2)^2 = (\alpha_1 + \alpha_2)(\beta_1 + \beta_2)s - (\mathbf{k}_1 + \mathbf{k}_2)_\perp^2 \simeq \alpha_1\beta_2 s = \mathcal{O}(s), \tag{12.10a}$$

$$s_{II} \equiv (p_1 - k_1 + p_2 - k_2)^2 \simeq (1 - \alpha_1)(1 - \beta_2)s = \mathcal{O}(s). \tag{12.10b}$$

This allows us to substitute the asymptotic Regge pole expression f_1 for the ladder amplitudes (12.9),

$$f_{1,I} \simeq g_{I,1} \cdot \xi_{\alpha(k^2)} s_I^{\alpha(k^2)} \cdot g_{I,2}, \tag{12.11a}$$

$$f_{1,II} \simeq g_{II,1} \cdot \xi_{\alpha((q-k)^2)} s_{II}^{\alpha((q-k)^2)} \cdot g_{II,2}, \tag{12.11b}$$

where

$$g_{I,1} = g(\mathbf{k}_\perp^2; k_1^2, (k_1 - k)^2), \quad g_{I,2} = g(\mathbf{k}_\perp^2; k_2^2, (k_2 + k)^2), \tag{12.11c}$$

and the residues of the second pole, $g_{II,i}$ in (12.11b), differ from (12.11c) by the substitution $k \rightarrow q - k$, $k_1 \rightarrow p_1 - k_1$ and $k_2 \rightarrow p_2 - k_2$.

As far as the dependence on the longitudinal components of the reggeon-loop momentum k is concerned, the factorization property (12.8) holds also for the Regge residues: the top residues $g_{I,1}$ and $g_{II,1}$ depend only on β_k , while the bottom ones, $g_{I,2}$ and $g_{II,2}$, only on α_k .

Given such a splitting of the dependence of the integrand on α_k and β_k variables, we can represent the original integral (12.4) in the following compact form,

$$f_2(s, q^2) = \frac{i}{2!} \int \frac{d^2\mathbf{k}_\perp}{(2\pi)^2} \xi_{\alpha(k^2)} \xi_{\alpha((q-k)^2)} s^{\alpha(k^2) + \alpha((q-k)^2) - 1} N_1 N_2. \tag{12.12a}$$

Here

$$N_1 = N(q^2; k^2, (q-k)^2) = \frac{1}{\sqrt{2}} \int \frac{d^4k_1}{(2\pi)^{4i}} \alpha_1^{\alpha(k^2)} (1 - \alpha_1)^{\alpha((q-k)^2)} \times \int \frac{s d\beta_k}{2\pi i} \frac{g(k_1, k)g(p_1 - k_1, q - k)}{(\)(\)(\)(\)}, \tag{12.12b}$$

with $(\)$ marking the four propagators written explicitly in (12.4). We have introduced the factor s in the β_k integral since from (12.7) we know that $\beta_k \propto 1/s$; so defined, N has a finite $s \rightarrow \infty$ limit. The expression for N_2 is similar to (12.12b) but with the internal integral running over α_k , instead of β_k . In fact, $N_1 = N_2$.

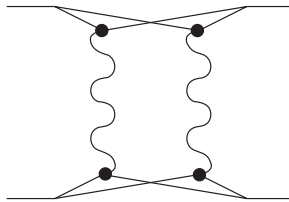
The factor $1/\sqrt{2}$ has emerged from the reggeon loop integral:

$$d^4k = \frac{s}{2} d\alpha_k d\beta_k d^2\mathbf{k}_\perp = d^2\mathbf{k}_\perp \cdot \left(\frac{s d\beta_k}{\sqrt{2}}\right) \cdot \left(\frac{s d\alpha_k}{\sqrt{2}}\right) \times \frac{1}{s}$$

(the last factor $1/s$ went into the shift of the energy exponent in (12.12a)).

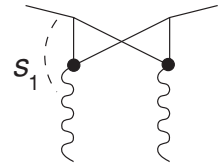
12.3 Analytic structure of the particle–reggeon vertex

What is the diagrammatic meaning of our exercise? We have replaced the ladder amplitudes by reggeons:



The function N contains an integral over the loop momentum k_1 of the product of four particle propagators and two reggeon vertices.

I would say that N describes the conversion of two particles into two reggeons, from the t -channel perspective, or the particle–reggeon scattering (in s channel). If I had to invent the corresponding amplitude A , it would depend on the energy of the ‘colliding objects’,



$$s_1 = (p_1 - k_1)^2 = (1 - \alpha_k)(\gamma - \beta_k)s \approx (\gamma - \beta_k)s.$$

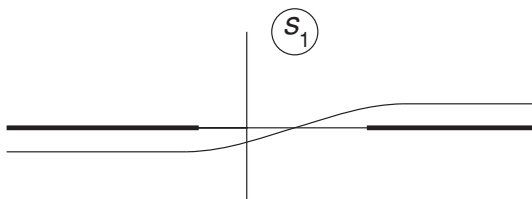
This relation tells us that β_k determines the particle–reggeon pair energy so that $sd\beta_k = -ds_1$. Taking this into account, we can write N as

$$N = \int_{-\infty}^{\infty} \frac{ds_1}{2\pi i} A(s_1, q^2; k^2, (q - k)^2), \tag{12.13}$$

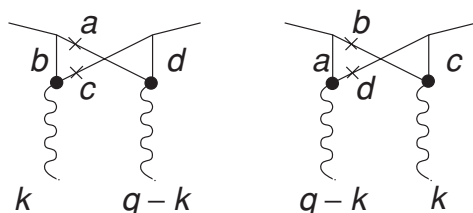
where the particle–reggeon scattering amplitude A depends on the ‘virtual masses’ of the reggeons $k^2, (q - k)^2$, apart from the standard s and $t = q^2$ variables.

It is easy to extract the structure of A from (12.12b). Its only unusual feature is the presence of the powers of α_1 and $(1 - \alpha_1)$ which factors have emerged from the reggeon energies (12.10). The origin of these factors can be understood as follows. If in the t -channel exchange we had a *particle* k with spin σ , the vertex would have had tensor structure, $k_{\mu_1} \dots k_{\mu_\sigma}$. Our expression contains, in fact, $(\cos)^{\alpha(k_\perp^2)}$; here $\alpha(k_\perp^2)$ plays the rôle of σ and ‘counts the number of tensor indices’.

Let us have a deeper look at the function N . In the complex plane of the energy variable s_1 , the amplitude A in (12.13) has cuts both at positive and negative s_1 :



These cuts are described by two diagrams



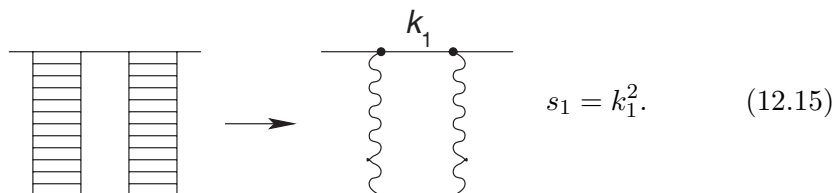
which differ by the exchange of the reggeon momenta ($s \leftrightarrow u$). By putting the particles a and c in the first graph on-mass-shell we get the right cut; cutting through b and d in the second graph corresponds to the left one.

We have here a curious expression: an integral of the amplitude over the energy. If the behaviour at $s_1 \rightarrow \infty$ is suitable (which is so for this concrete diagram which decreases well), the contour can be closed, say, around the right cut and we get a finite, real answer for N :

$$N = \int_{s_0}^{\infty} \frac{ds_1}{\pi} A_1(s_1). \tag{12.14}$$

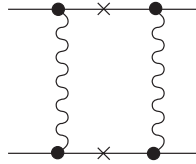
12.3.1 Amati–Fubini–Stanghellini puzzle

Let us return to the diagram of Fig. 12.1(b) which I did not like from the point of view of the space–time consideration. Repeating the above procedure literally, we arrive at a picture with a single particle separating two reggeons:



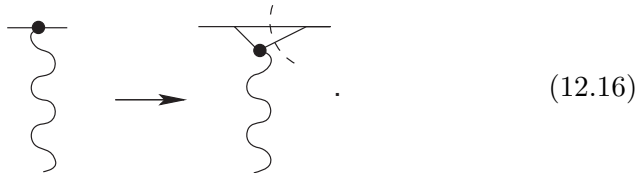
Amati, Fubini and Stanghellini (AFS) have considered elastic scattering and stated that there were branchings generated by the following

two-reggeon diagram

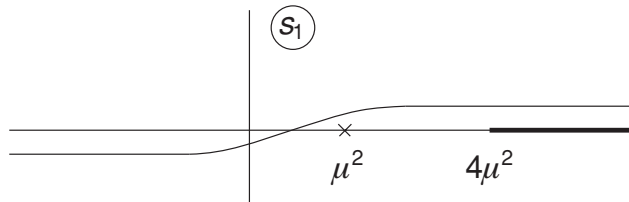


Indeed, if the reggeon residue g were a constant, we would get a finite answer $N \propto g^2$ coming from $A_1(s_1) = \pi g^2 \delta(s_1 - \mu^2)$.

However, $g(s_1) \neq \text{const}$, since the vertex contains various singularities reflecting the dependence on the virtuality $k_1^2 \equiv s_1$,

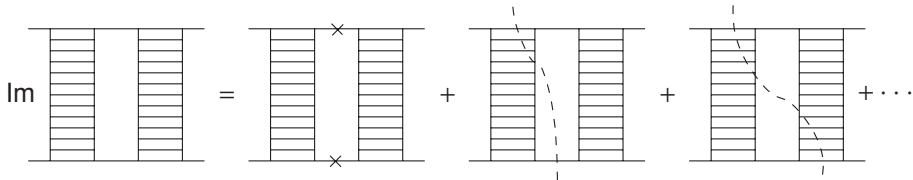


Because of this, N will have a *right cut* apart from the pole at $s_1 = \mu^2$:



The main question is, how g behaves – does it decrease with k_1^2 ? If yes, we can close the contour *to the left* and get $N=0$. This is so in all reasonable theories (in $\lambda\varphi^3$, for example; in any case, we are actually interested in those theories in which the transverse momenta are limited).

It is interesting to see how N disappears. When we calculate the imaginary part of the AFS diagram,



each discontinuity, corresponding to a definite cut on the r.h.s., is different from zero. The first contribution is obviously positive. The other have alternating signs and correspond, in fact, to cutting through the vertex (or simultaneously two vertices) as in (12.16). We see an astonishing picture: each specific cut of the amplitude decreases slowly with s , while the whole amplitude falls fast and does not contribute in the high-energy limit due

to $N=0$. According to Mandelstam, there are branchings, indeed, but they are different from (12.15).

To understand the mechanism of the vanishing of the AFS graph is very important. It teaches us how analytic properties of Feynman diagrams are related to the space–time picture of the s -channel processes.

Let us return to the general case and represent the particle–reggeon scattering amplitude as a sum of right- and left-cut contributions:

$$A(s_1) = \frac{1}{\pi} \int_{\text{right}} \frac{ds'_1 A_1(s'_1)}{s'_1 - s_1} + \frac{1}{\pi} \int_{\text{left}} \frac{ds'_1 A_2(s'_1)}{s'_1 - s_1}. \tag{12.17}$$

Now substitute into the integral (12.13) for N the right- and left-cut contribution, separately. We could, it seems, close the contour to the *left* in the s_1 -integral of the first (right cut) term, to the *right* of the second (left cut) one, and get $N=0 + 0$. When would such a trick not work? We will have $N \neq 0$ in the only case when the *separate* contributions of two cuts do not decrease faster than $1/s_1$ on the large circle, $|s_1| \rightarrow \infty$. But these are just those diagrams (see section 1 of this lecture) which possess a *third spectral function* ρ_{su} .

Let us recall that it was actually the third spectral function which led us to a contradiction with the Regge pole picture: a problem of the partial wave having the pole at $\ell = -1$ emerged.

In a way, here the circle closes. Both from the t -channel and the s -channel we came to the conclusion that the reggeon branching emerges only in the *relativistic theory*, where we have $\rho_{su} \neq 0$ which guarantees a non-vanishing contribution, $N \neq 0$. This corresponds to diagrams in which the singularities in s and u cannot be separated.

12.3.2 Reggeon branching contribution to cross section

Finally, let us calculate f_2 given in (12.12) to see whether it corresponds indeed to a two-reggeon branching as we expect. For positive signature, at small transverse momenta where $\alpha \simeq 1$ we have

$$\xi_\alpha = -\frac{1 + e^{-i\pi\alpha}}{\sin \pi\alpha} = \frac{-e^{-i\frac{\pi\alpha}{2}}}{\sin \frac{\pi\alpha}{2}} \simeq i.$$

Since the integrand in (12.12a) contains an exponential factor

$$\exp\{(\alpha(k^2) + \alpha((k - q)^2)) \ln s\},$$

at large $\ln s$ the answer will be dominated by the value of the transverse momentum at which the exponent is maximal, and can be evaluated by

the steepest-descent method. In the linear approximation,

$$\begin{aligned} \alpha(k^2) + \alpha((k - q)^2) - 2\alpha(0) &\simeq -\alpha'(\mathbf{k}_\perp^2 + (\mathbf{k} - \mathbf{q})_\perp^2) \\ &= -\frac{1}{2}\alpha'\mathbf{q}_\perp^2 - 2\alpha'(\mathbf{k} - \frac{1}{2}\mathbf{q})_\perp^2, \end{aligned}$$

the \mathbf{k}_\perp integration yields

$$\int \frac{d^2\mathbf{k}_\perp}{(2\pi)^2} e^{-\alpha'(\mathbf{k}_\perp^2 + (\mathbf{k} - \mathbf{q})_\perp^2) \ln s} = \frac{1}{8\pi \ln s} e^{-\frac{1}{2}\alpha'\mathbf{q}_\perp^2 \ln s}.$$

Observing that

$$2\alpha(0) - 1 + \frac{1}{2}\alpha't \simeq 2\alpha(t/4) - 1, \quad t \equiv q^2 = -\mathbf{q}_\perp^2,$$

we finally arrive at

$$f_2(s, t) \simeq i \xi_{\alpha(t/4)}^2 N^2 \frac{s^{2\alpha(t/4)-1}}{16\pi\alpha' \ln s}; \quad N = N(q/2, q/2). \tag{12.18}$$

The result of our s -channel calculation is perfectly satisfactory: the $(\ln s)^{-1}$ suppression tells us that we have indeed found a branch-cut singularity. Its position in the j -plane follows the Mandelstam rule (11.36); the sign of this expression is also correct: $\text{Im } f_2 \propto \xi_\alpha^2 = -1$ (N is real).

12.3.3 Branching in the impact parameter space

At small t the two-reggeon contribution is suppressed as $1/\ln s$ as compared to the pomeron pole. It is easy to understand the origin of this suppression, if we turn to the impact parameter space. The image of the pole amplitude is

$$f_1(s, q^2) \simeq i s g^2 e^{-\alpha'\mathbf{k}^2\xi} \equiv i s g^2 \int d^2\rho e^{i\mathbf{k}\cdot\rho} G_1(\rho, \xi); \tag{12.19a}$$

$$G_1(\rho, \xi) = \frac{e^{-\rho^2/4\alpha'\xi}}{4\pi\alpha'\xi}, \quad \xi \equiv \ln s. \tag{12.19b}$$

Let us evaluate the Fourier transform of the two-pomeron branching:

$$s \cdot G_2(\rho, \xi) \equiv \int \frac{d^2\mathbf{q}}{(2\pi)^2} e^{-i\mathbf{q}\cdot\rho} f_2(s, q^2). \tag{12.20}$$

Substituting (12.19) in the amplitude (12.12),

$$\int \frac{d^2\mathbf{q}}{(2\pi)^2} \frac{d^2\mathbf{k}}{(2\pi)^2} e^{-i\mathbf{q}\cdot\rho} e^{i\mathbf{k}\cdot\rho_1 + i(\mathbf{q}-\mathbf{k})\cdot\rho_2} G_1(\rho_1, \xi) G_1(\rho_2, \xi) N^2 d^2\rho_1 d^2\rho_2,$$

the integrals over momenta produce $\rho_1 = \rho_2 = \rho$, and we derive

$$G_2(\rho, \xi) = -i N^2 G_1^2(\rho, \xi). \tag{12.21}$$

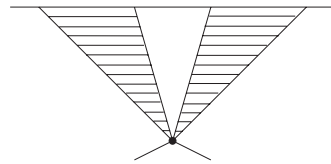
The pole amplitude (12.19b) describes *two-dimensional diffusion* in the impact parameter space. It gives the probability to find a particle (placed at $\rho=0$ at zero time) in a given point ρ after the time ξ (α' determines the diffusion rate). In this language, the expression (12.21) corresponds to finding *two particles* in the same point. It is clear that such a probability is inverse proportional to the area and decreases with time, $1/S \propto 1/\alpha'\xi$. This can be seen directly by integrating (12.21) over ρ :

$$f_2(t=0) \propto \int d^2\rho G_2(\rho, \xi) \propto \frac{1}{\xi}, \quad \text{while } f_1(t=0) \propto \int d^2\rho G_1(\rho, \xi) = 1.$$

12.4 Branchings in quantum mechanics: screening

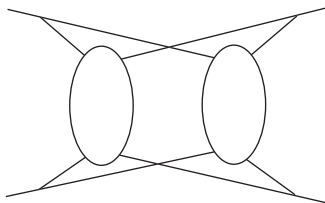
We got the reggeon branchings from the Mandelstam diagrams with ‘crosses’ in both vertices (Fig. 12.2(a)). In the previous section we have analysed the rôle of the third spectral function and understood, why a simpler picture, that of Fig. 12.2(b), would not produce a branch cut in the j -plane.

What is the difference between the two pictures? In the second case, the particle moves as an elementary object just repeating the interaction. As we have discussed above, the probability of such a process cannot be significant since the multi-particle fluctuation (‘ladder’) does not have enough time to collapse back into a single particle before it experiences the second scattering.

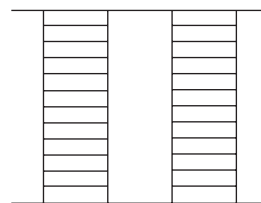


What is shown in the diagram of Fig. 12.2(a)?

Let us look at the lower part of the graph. Here the scattering occurs not on an elementary object, as in the diagram (b), but on the *decay products* of the target particle. We can model this picture in the non-relativistic



(a)



(b)

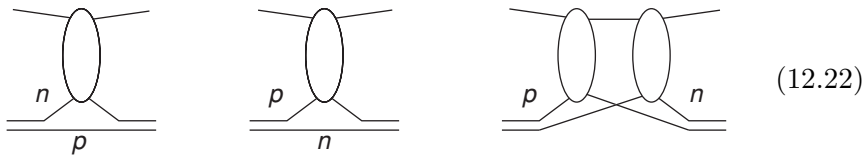
Fig. 12.2 Mandelstam two-reggeon branching (a) and the AFS graph (b).

scattering theory language if we take a deuteron D – a pn bound state – and study the scattering of the projectile off the proton and the neutron inside D .

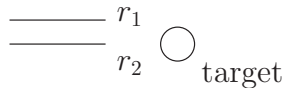
There is a subtle point: in the relativistic theory both the upper and the lower parts of the diagram have to be complex – have to have ‘crosses’. However, we will ignore this detail for the time being and consider the pion–deuteron scattering in non-relativistic quantum mechanics.

12.4.1 Deuteron scattering

Graphically, there are three possibilities for the πD scattering:



Since what happens in the upper part does not concern us for the time being, we can look upon this process as a scattering of a deuteron in the external potential (of the target pion).

Assume that a fast deuteron hits a potential:  target

How would I calculate this process quantum-mechanically?

In the initial state we have the wave function

$$\psi(\mathbf{r}_1, \mathbf{r}_2) = e^{i\mathbf{p}\cdot\frac{1}{2}(\mathbf{r}_1+\mathbf{r}_2)}\psi_D(\mathbf{r}_{12}), \quad \mathbf{r}_{12} = \mathbf{r}_1 - \mathbf{r}_2, \tag{12.23}$$

where \mathbf{p} is the deuteron momentum, and $\psi_D(\mathbf{r}_{12})$ describes the relative motion of the proton p and neutron n inside it.

When D flies fast, it is clear that its nucleons have no time to interact with each other, so that the potential acts on p and n independently. Then in the final state the wave function acquires the scattering phase given by the sum of the p and n scattering phases:

$$\psi(\mathbf{r}_1, \mathbf{r}_2) \rightarrow \psi'(\mathbf{r}_1, \mathbf{r}_2) = \psi(\mathbf{r}_1, \mathbf{r}_2) e^{2i\delta(\boldsymbol{\rho}_1)+2i\delta(\boldsymbol{\rho}_2)}.$$

The phase depends on the impact parameters of the nucleons in the deuteron, $\boldsymbol{\rho}_1$ and $\boldsymbol{\rho}_2$, which do not change (stay ‘frozen’) in the course of the high-energy scattering.

To calculate the amplitude, I have to project ψ' onto the final state wave function ψ_f with a given momentum $\mathbf{p}_f = \mathbf{p} + \mathbf{q}$. If we are interested in D in the final state, we take $\psi_f = \psi_D$; if we investigate the decay, we look

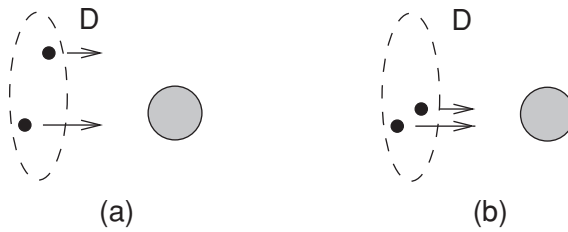


Fig. 12.3 Independent scattering (a) and shadowing configurations (b).

for $\psi_p\psi_n$. Since the S -matrix element does not depend on the longitudinal coordinates, \mathbf{z}_i , the momentum transfer is purely transversal, $\mathbf{q} = \mathbf{q}_\perp$.

To derive the following expression is a very useful exercise (-1 subtracts the incoming beam):

$$f = \frac{p}{i} \int \frac{d^2\rho_c}{2\pi} e^{i\mathbf{q}_\perp \cdot \rho_c} \int d^3\mathbf{r}_{12} \psi_f^*(\mathbf{r}_{12}) [e^{2i\delta(\rho_1)+2i\delta(\rho_2)} - 1] \psi_D(\mathbf{r}_{12}). \tag{12.24}$$

Let us take D in the final state and consider the forward scattering amplitude, $\mathbf{q}_\perp = 0$:

$$f(0) = ip \int \frac{d^2\rho_c}{2\pi} \int \psi_D^*(\mathbf{r}_{12}) [1 - e^{2i(\delta_1+\delta_2)}] \psi_D(\mathbf{r}_{12}) d^3\mathbf{r}_{12}. \tag{12.25}$$

At the first glance nothing in the expression (12.25) resembles the diagrams of (12.22).

What is the difference between the two approaches?

The quantum-mechanical expression contains no information on which of the two particles has actually interacted and which has not, while in the language of Feynman graphs this is the main thing that enters.

To relate the two approaches, let us look at the simple algebraic identity

$$1 - S_1S_2 = (1 - S_1) + (1 - S_2) - (1 - S_1)(1 - S_2), \quad S_i = e^{2i\delta(\rho_i)}. \tag{12.26}$$

It can be interpreted as follows. The first two terms $(1 - S)$ describe independent interactions of p and n with the potential; the presence of the third one tells us that the sum of independent contributions apparently overestimates the answer, over-counts something. Indeed, when *one* of the nucleons interacts with the target as in Fig. 12.3(a), we get a sum of two contributions to the cross section.

However, the deuteron may also hit the potential in the configuration shown in Fig. 12.3(b). Here *both* nucleons interact though this contribution should be counted only once in the total cross section. It is the rôle of the quadratic term in (12.26) to correct for the double counting of the

deuteron configuration in which one of the nucleons is *screened* by the other. It is clear therefore that this term – the ‘shadowing correction’ – must enter with a minus sign in the total cross section, related to the forward amplitude by the optical theorem,

$$\sigma_{\text{tot}} = \frac{4\pi}{p} \text{Im} f(0). \quad (12.27)$$

The magnitude of the shadowing depends entirely on the geometry of the scattering process, on the size of the deuteron r_D as compared to the size of the potential, R . Let us analyse the two extreme cases.

$R \gg r_D$. This is the case of a very *broad* target. The total deuteron cross section, $\sigma_{\text{tot}} = 2\pi R^2$, will emerge from (12.26) as

$$2\pi R^2 = 2\pi R^2 + 2\pi R^2 - 2\pi R^2, \quad (12.28a)$$

meaning that the shadowing is 100% strong.

$R \ll r_D$. In this case the shadowing will occur only when the proton and neutron happen to have the same impact parameter, $|\boldsymbol{\rho}_1 - \boldsymbol{\rho}_2| \lesssim r_D$. The geometric weight of such rare configurations translates into a small shadowing correction

$$\frac{\Delta\sigma}{\sigma_1} \propto \frac{R^2}{r_D^2} \ll 1. \quad (12.28b)$$

12.4.2 Broad target

Consider first the case of a large target. One may have in mind, e.g. deuteron scattering off a heavy nucleus A , $A^{1/3} \propto R \gg r_D$. We obtain a big cross section by integrating the deuteron impact parameter $\boldsymbol{\rho}_c$ over the large area, $|\boldsymbol{\rho}_c| < R$. In this situation we can neglect the dependence on the relative coordinate, $\boldsymbol{\rho}_{12} = \boldsymbol{\rho}_1 - \boldsymbol{\rho}_2$, and approximate

$$\delta_1 = \delta(\boldsymbol{\rho}_c + \frac{1}{2}\boldsymbol{\rho}_{12}) \simeq \delta_2 = \delta(\boldsymbol{\rho}_c - \frac{1}{2}\boldsymbol{\rho}_{12}) \simeq \delta(\boldsymbol{\rho}_c).$$

Since in this approximation the S -matrix does not depend on \mathbf{r}_{12} , we get

$$f(0) = ip \int \frac{d^2\boldsymbol{\rho}_c}{2\pi} \left(1 - e^{4i\delta(\boldsymbol{\rho}_c)}\right) \times 1, \quad (12.29)$$

where the last ‘1’ originates from the wave function normalization,

$$\int d^3\mathbf{r}_{12} |\psi_D(\mathbf{r}_{12})|^2 = 1. \quad (12.30)$$

If a deuteron hits a big nucleus head-on, it definitely interacts and disappears (is absorbed), feeding various inelastic channels. This corresponds

to the elasticity coefficient $\eta(\boldsymbol{\rho})$ in the S -matrix element being vanishingly small at $|\boldsymbol{\rho}| < R$, so that

$$e^{2i\delta(\boldsymbol{\rho})} \equiv \eta(\boldsymbol{\rho}) e^{2i\beta(\boldsymbol{\rho})} \simeq \begin{cases} 0, & \text{for } |\boldsymbol{\rho}| < R, \\ 1, & |\boldsymbol{\rho}| \gg R. \end{cases}$$

This is the ‘black disc’ picture,

$$\int_0^\infty \frac{d^2 \boldsymbol{\rho}_c}{2\pi} (1 - e^{4i\delta(\boldsymbol{\rho}_c)}) \simeq \int_0^R \frac{d^2 \boldsymbol{\rho}_c}{2\pi} \simeq \frac{1}{2} R^2,$$

yielding the total cross section

$$\sigma_{\text{tot}} = \frac{4\pi}{p} \text{Im } f(0) \simeq 2\pi R^2.$$

Half of this cross section is the diffractive elastic scattering,

$$\sigma_{\text{el}} = \int d\Omega |f(q)|^2 = \int d^2 \mathbf{q} \frac{|f(q)|^2}{p^2} = \int d^2 \boldsymbol{\rho} |1 - e^{4i\delta(\boldsymbol{\rho})}|^2 \simeq \pi R^2;$$

the other half is due to *inelastic* processes.

12.4.3 Diffractive dissociation of a deuteron

What if I am interested not in the elastic scattering, but in the deuteron break-up $D \rightarrow pn$? In principle, this is one of the inelastic channels. We are, however, interested in the specific inelastic process in which the target nucleus remains intact and scatters as a whole, $D + A \rightarrow p + n + A$, instead of being ‘heated up’.

Such a *diffractive dissociation* of the deuteron is possible only if the momentum transfer is very small, $q \sim R^{-1}$, corresponding to scattering angles $\theta_s \sim 1/pR$; otherwise the nucleus A would break up too.

What will be the scale of such a cross section? Obviously, its amplitude cannot be as large as the elastic one. If it were, integrating over the same narrow angular cone as for the elastic scattering, we would get a diffractive dissociation cross section $\sigma_{\text{tot}}^{\text{dd}}$ as large as the elastic one:

$$\sigma_{\text{tot}}^{\text{dd}} = \int |f_{D \rightarrow pn}|^2 d\Omega \sim \int d\theta_s^2 |pR^2|^2 \sim R^2, \quad d\theta_s^2 \sim \frac{1}{(pR)^2}.$$

But there is no place left in σ_{tot} to accommodate another contribution of the order of R^2 . What is going on in the formula?

The point is that in the rough approximation of the scattering phases independent of $\boldsymbol{\rho}_{12}$, the main term in the forward scattering amplitude, $\mathbf{q} = 0$, cancels because of the *orthogonality of the initial- and final-state*

wave functions:

$$f_{D \rightarrow pn}(0) = \frac{ip}{2\pi} \int d^2 \rho_c [1 - S_1 S_2] \cdot \langle \psi_{pn} | \psi_D \rangle; \quad (12.31)$$

$$\langle \psi_{pn} | \psi_D \rangle = \int d^3 \mathbf{r}_{12} \psi_{pn}^*(\mathbf{r}_{12}) \psi_D(\mathbf{r}_{12}) = 0.$$

To prevent this cancellation, the expansion of the phase in ρ_{12} has to be carried out,

$$\delta[1 - S_1 S_2] \simeq \frac{1}{4} [(\rho_{12} \nabla_{\rho_c} S)^2 - S(\rho_{12} \nabla_{\rho_c} S)^2], \quad S = S(\rho_c). \quad (12.32)$$

If S changes smoothly, $|\nabla S| \sim R^{-1}$, then

$$p^{-1} f_{D \rightarrow pn}(0) \sim \int^R \rho_c d\rho_c \frac{\langle \psi_{pn} | \rho_{12}^2 | \psi_D \rangle}{R^2} \sim r_D^2. \quad (12.33)$$

If the target has a relatively *sharp edge*, in which region S only changes, the forward amplitude gets enhanced,

$$p^{-1} f_{D \rightarrow pn}(0) \sim \int \rho_c d\rho_c \frac{\delta(\rho_c - R)}{H} \cdot r_D^2 \sim \frac{R}{H} \cdot r_D^2, \quad (12.34)$$

where $H \sim 1/\mu$ is the width of the transition region, $R \gg H \gg r_D$. In this case the inelastic amplitude is still suppressed as $1/R \propto A^{-1/3}$ as compared to the elastic one.

The nature of the suppression of the forward dissociation amplitude (12.34) is consistent with the total contribution of inelastic diffraction to the interaction cross section, $\sigma_{\text{tot}}^{\text{dd}}$. When we take $\mathbf{q} \neq 0$ in the transition amplitude (12.24), the wave functions are no longer orthogonal; for small \mathbf{q} one has

$$\langle \psi_{pn}(\mathbf{p} + \mathbf{q}) | \psi_D(\mathbf{p}) \rangle \sim (\mathbf{q} \cdot \mathbf{k}_{pn}) r_D^2,$$

where \mathbf{k}_{pn} is the relative momentum of the nucleons. Integrating the amplitude squared over the scattering angle, one obtains

$$\int \frac{d^2 \mathbf{q}}{p^2} |f_{D \rightarrow pn}|^2 \sim r_D^4 \int d^2 \rho_c |(\mathbf{k}_{pn} \cdot \nabla_{\rho_c} S^2)|^2 \sim \pi R \cdot \frac{r_D^2}{H} \cdot \mathbf{k}_{pn}^2 r_D^2.$$

An integral over \mathbf{k}_{pn} produces $\langle \mathbf{k}_{pn}^2 \rangle r_D^2 \sim 1$, and we get the estimate

$$\sigma_{\text{tot}}^{\text{dd}} \sim \pi R \cdot \frac{r_D^2}{H},$$

consistent with the magnitude of the forward amplitude (12.34).

Diffraction dissociation occurs only on the *periphery* of the target nucleus. It is very important to understand that the diffraction does not

change the internal state of the system, unless the system is scattered as a whole, $\mathbf{q}_\perp \neq 0$.

12.4.4 Shadowing

We return to the discussion of the shadowing correction. Combining (12.24) and (12.26), we have

$$f(\mathbf{q}) = \frac{ip}{2\pi} \int d^2 \boldsymbol{\rho}_c e^{i\mathbf{q}\boldsymbol{\rho}_c} \left\langle (1-S_1) + (1-S_2) - (1-S_1)(1-S_2) \right\rangle, \quad (12.35)$$

where $\langle \ \rangle$ stands for the average over the deuteron state. Let us consider this expression term by term, $f = f_1 + f_2 + f_{12}$. Recall that $S_1 = S_1(\boldsymbol{\rho}_1) = S_1(\boldsymbol{\rho}_c + \frac{1}{2}\boldsymbol{\rho}_{12})$. Introducing the Fourier transform of the profile of the nucleon scattering matrix element,

$$1 - S_1(\boldsymbol{\rho}) = \int \frac{d^2 \mathbf{k}}{(2\pi)^2} e^{-i\mathbf{k}\cdot\boldsymbol{\rho}} \varphi_1(\mathbf{k}),$$

and performing the impact parameter integrals we have

$$f_1(\mathbf{q}) = \frac{ip}{2\pi} \varphi_1(\mathbf{q}) \cdot F_D(\mathbf{q}^2), \quad (12.36)$$

where F is the *electromagnetic charge form factor* of the deuteron, given by the Fourier transform of the probability density to find the electric charge (proton) inside the deuteron:

$$F_D(\mathbf{q}^2) = \int d^3 \mathbf{r}_{12} |\psi_D(\mathbf{r}_{12})|^2 e^{-i\frac{\mathbf{q}}{2}\cdot\mathbf{r}_{12}}; \quad F(0) = 1.$$

The optical theorem (12.27) tells us that $\varphi(0)$ is simply related to the total interaction cross section of a single nucleon with the target,

$$\varphi(0) = \frac{1}{2} \sigma_N. \quad (12.37)$$

For the last term in (12.35) we have

$$(1-S_1)(1-S_2) = \int \frac{d^2 \mathbf{k}_1}{(2\pi)^2} \frac{d^2 \mathbf{k}_2}{(2\pi)^2} \varphi_1(\mathbf{k}_1) \varphi_2(\mathbf{k}_2) e^{-i(\mathbf{k}_1+\mathbf{k}_2)\boldsymbol{\rho}_c} e^{-i\frac{\mathbf{k}_1-\mathbf{k}_2}{2}\boldsymbol{\rho}_{12}},$$

and derive analogously

$$f_{12}(\mathbf{q}) = -\frac{ip}{2\pi} \int \frac{d^2 \mathbf{k}}{(2\pi)^2} \varphi_1(\frac{1}{2}\mathbf{q} + \mathbf{k}) \varphi_2(\frac{1}{2}\mathbf{q} - \mathbf{k}) \cdot F_D(4\mathbf{k}^2). \quad (12.38)$$

Assembling the three terms of (12.35), for the total cross section we obtain

$$\sigma_D = \sigma_p + \sigma_n - 2 \operatorname{Re} \int \frac{d^2 \mathbf{k}}{(2\pi)^2} \varphi_p(\mathbf{k}) \varphi_n(-\mathbf{k}) \cdot F_D(4\mathbf{k}^2). \quad (12.39)$$

Now we are ready to check our expectations (12.28) about the magnitude of the shadowing correction that were based on the classical geometric considerations.

Broad potential. In this case p and n almost always hit the target together, and we expected in (12.28a) a 100% negative shadowing correction. Within the black-disc model, the nucleon amplitude f_1 is purely imaginary, so that φ is real and we can replace $\text{Re } \varphi^2$ by $|\varphi|^2$. Using

$$\frac{|\varphi(\mathbf{k})|^2}{(2\pi)^2} = \frac{1}{p^2} |f_1(\mathbf{k})|^2 = \frac{1}{p^2} \frac{d\sigma_{\text{el}}^N}{d\Omega} \simeq \frac{d\sigma_{\text{el}}^N}{d^2\mathbf{k}},$$

this allows us to represent (12.39) in terms of the differential elastic nucleon scattering cross section as

$$\sigma_{\text{tot}}^D = 2\sigma_{\text{tot}}^N - 2 \int d\mathbf{k}^2 \frac{d\sigma_{\text{el}}^N}{d\mathbf{k}^2} F_D(4\mathbf{k}^2). \quad (12.40)$$

The characteristic momenta in the integral (12.40), $\mathbf{k}^2 \sim R^{-2}$ are much smaller than the internal scale of the form factor, r_D^{-2} , therefore we can put $F = F(0) = 1$ to obtain

$$\sigma_{\text{tot}}^D = 2\sigma_{\text{tot}}^N - 2\sigma_{\text{el}}^N = 2\sigma_{\text{tot}}^N - \sigma_{\text{tot}}^N = \sigma_{\text{tot}}^N.$$

Compact potential, large-size projectile. The product $\varphi_p(\boldsymbol{\rho}_1)\varphi_n(\boldsymbol{\rho}_2)$ requires p and n to be at the same impact parameter in order to simultaneously aim at the small-size target, $R \ll r_D$, and screen one another. The deuteron form factor falling sharply above $\mathbf{k}^2 \sim r_D^{-2} \ll R^{-2}$, the factors φ in (12.39) can be taken out,

$$\sigma_D \simeq \sigma_p + \sigma_n - 2\varphi_p(0)\varphi_n(0) \int \frac{d\mathbf{k}^2}{4\pi} F_D(4\mathbf{k}^2).$$

Invoking (12.37), this immediately gives the Glauber formula

$$\sigma_D \simeq \sigma_p + \sigma_n - \frac{\sigma_p\sigma_n}{4\pi} \cdot \overline{r_D^{-2}}, \quad (12.41a)$$

where we have used

$$\overline{r_D^{-2}} \equiv \int d^3\mathbf{r}_{12} \frac{|\psi_D(\mathbf{r}_{12})|^2}{\mathbf{r}_{12}^2} = \frac{1}{2} \int d\mathbf{k}^2 F_D(4\mathbf{k}^2). \quad (12.41b)$$

12.5 Back to relativistic theory

The analogy between the quantum-mechanical shadowing phenomenon and the two-reggeon branching can be made explicit if we substitute the

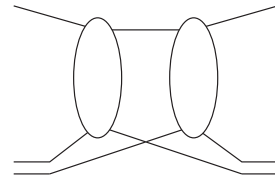
relativistic amplitude in the expression (12.38) for the double-scattering graph:

$$2i\varphi_1(\mathbf{q}) = \frac{4\pi f_1(\mathbf{q})}{p} \implies \frac{A(s, t)}{s}.$$

We have used the deuteron as a model for a composite target, in order to understand the origin of the negative correction due to the exchange of two reggeons. Let us say a few words about the real deuteron, about high-energy πD scattering.

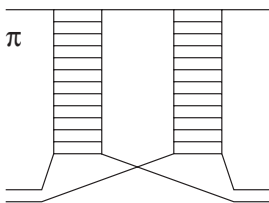
12.5.1 Glauber scattering

We have analysed the double scattering in quantum mechanics and found a large correction. We could carry out this calculation directly from relativistic diagrams, in the non-relativistic approximation (treating the masses of the particles as large parameters).



But, in the framework of our former logic, this correction has to be *zero*, since there is *no cross* in the upper part of the corresponding diagram! On the other hand, the non-zero answer was legitimately obtained in the non-relativistic theory. What is happening here?

Normally there are no small parameters in the diagrams describing relativistic hadron interactions. The deuteron problem is, however, special: calculating the diagrams for πD scattering we encounter a *small parameter*, namely the ratio of the size of the pion, $R \sim r_0 \sim \mu^{-1}$, to that of the deuteron, $R/r_D \ll 1$. It is the presence of this new parameter that is responsible for the survival of the *semi-AFS* diagram.



What is the reason for that, in classical terms? Consider the process in a reference frame in which the π meson is fast. Assuming that the situation is non-relativistic, we have obtained three contributions: π collided with either of p or n , or there was screening as a result of a double interaction. Why were

there no virtual particles involved; why was the answer expressed via the on-mass-shell amplitudes, i.e. via real particles?

We assumed r_D to be large, and this was the reason why, in the non-relativistic theory, π propagated between the two successive collisions as a real particle. The fact that the π meson had to pass a large distance, limited the energy uncertainty, $\Delta E \sim 1/\Delta t \sim 1/r_D \ll 1/R \sim \mu$, and forced π to be real. But this argument disregards the relativistic retardation

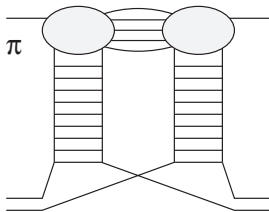
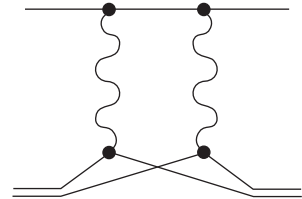
effect (as if virtual objects could not propagate at large distances!). In the relativistic situation, $E_\pi \gg \mu$, the lifetime of the virtual pion fluctuation, $\Delta t \sim E_\pi/(\Delta m)^2$, may become comparable with r_D even for large invariant masses of the virtual state, Δm . Depending on the pion energy, we have three scenarios.

- (1) $E/\mu^2 \ll r_D$. There is just one π , and the non-relativistic quantum mechanics gives a correct answer.
- (2) $E/\mu^2 \sim r_D$. A transitional regime: the pion can be accompanied by a small number of additional particles.
- (3) $E/\mu^2 \gg r_D$. In the space between the collisions with p and n , multi-particle showers with large invariant masses $(\Delta m)^2 \gg \mu^2$ can propagate, and the probability of just one π becomes vanishingly small.

12.5.2 Relativistic inelastic corrections to Glauber scattering

The deuteron example shows that the vertex blocks N that we have treated as constant, may contain, in specific cases, small internal parameters (like the deuteron binding energy) and therefore may still be changing fast at small momenta, well below a typical hadronic scale $\mathbf{k}^2 \lesssim \mu^2$.

There is another very important lesson. In the non-relativistic theory the screening means that one particle is an obstacle for another one just geometrically, i.e. the screening is the result of the geometry of subsequent collisions. It looks natural to discuss the scattering of a particle off a *nucleus* in terms of successive interactions with nucleons. In so doing, it is usually implied that the projectile preserves its identity when it propagates between successive collisions. This picture takes into account the Glauber corrections due to *elastic screening*. In the reggeon language, these diagrams correspond to *non-enhanced branchings*.



In the relativistic case there may be a whole shower propagating between the interaction points, since when the energy of the projectile $E \rightarrow \infty$, it itself fluctuates at distances exceeding the size of the target. We get another contribution to the screening phenomenon – an *inelastic screening*.

At very high energies the processes with large cascades become dominant. But these are again 'ladders'. Summing up high-mass intermediate inelastic states we arrive at the *enhanced branchings*,

